

J. Javier Brey · M.J. Ruiz-Montero

Average energy and fluctuations of a granular gas in the threshold of the clustering instability

Received: date

Abstract The behavior of an isolated dilute granular gas near the threshold of its clustering instability is investigated by means of fluctuating hydrodynamics and the direct simulation Monte Carlo method. The theoretical predictions from the former are shown to be in good agreement with the simulation results. The total energy of the the system is renormalized by the fluctuations of the vorticity field. Moreover, the scaled second moment of the energy fluctuations exhibits a power-law divergent behavior

Keywords Homegeous cooling state · clustering instability · critical behavior

1 Introduction

Granular materials often exhibit flows that are similar to those found in molecular fluids. In fact, phenomenological hydrodynamic-like equations are frequently used to describe them [1]. Nevertheless, in general, fluctuations of the hydrodynamic fields are much larger in granular systems than in ordinary fluids [2], as a consequence of the number of particles being many orders of magnitude smaller in the former than in the latter. Thus fluctuations are expected to play a more significant role in granular flows than in molecular fluid flows. In addition, it must be realized that a new source of noise and fluctuations is present in granular systems, associated with the localized character of the energy dissipation. The properties of this intrinsic noise remain largely unknown, although

J.J. Brey
 Física Teórica, Universidad de Sevilla, Apartado de Correos 1065. 41080 Sevilla. Spain
 Tel.: +34-954550936
 E-mail: brey@us.es

M.J. Ruiz-Montero
 Física Teórica, Universidad de Sevilla, Apartado de Correos 1065. 41080 Sevilla. Spain
 E-mail: majose@us.es

some simple limiting cases have been recently investigated [3; 4].

Here, some results for the total energy fluctuations in a freely evolving granular gas, below the critical size for the onset of the clustering or shear instability [5], will be reported. The model considered is a system of N smooth inelastic hard spheres of mass m and diameter σ . The inelasticity is assumed to be described by a constant, velocity independent, coefficient of normal restitution α . It is well known that the simplest possible state for this system is the so-called homogeneous cooling state (HCS). At the level of hydrodynamics, this state is described by a constant number density n_h , a vanishing flow velocity, and a time dependent temperature $T_h(t)$, that obeys the equation

$$\partial_t T_h(t) = -\zeta_h(t) T_h(t), \quad (1)$$

where $\zeta_h[n_h, T_h(t)]$ is a cooling rate that must be specified from a microscopic theory. For the case of hard spheres considered here, there is no microscopic energy scale associated with the collision model. Therefore, the temperature dependence of the cooling rate can be determined by dimensional arguments as $\zeta_h(t) \propto T_h^{1/2}(t)$. The HCS is unstable against long wavelength spatial perturbations, leading to the formation of velocity vortices and high density clusters of particles [5]. Linear stability analysis of the hydrodynamic equations indicates that this instability is driven by the transversal shear mode [5; 6]. Using phenomenological Navier-Stokes equations, it is found that the critical wavelength L_c beyond which the system becomes unstable is given by

$$L_c = 2\pi \left(\frac{2\eta^*}{\zeta^*} \right)^{1/2} \ell_0. \quad (2)$$

Here, $\ell_0 \equiv (n_h \sigma^2)^{-1}$ is proportional to the mean free path,

$$\zeta^* \equiv \frac{\zeta_h(t) \ell_0}{v_h(t)}, \quad (3)$$

and

$$\eta^* \equiv \frac{\eta(T_h)}{mn_h \ell_0 v_h(t)}, \quad (4)$$

where $v_h(t) \equiv [2T_h(t)/m]^{1/2}$ is a thermal velocity and $\eta(T_h)$ is the shear viscosity of the granular fluid. For the particular case of a dilute gas described by the inelastic Boltzmann equation, which is the case to be considered in the following, the explicit expressions of η and $\zeta_h(t)$ are given in [7].

Although the initial set up of the clustering instability has been extensively studied, much less attention has been paid to the behavior of the system as the instability is approached from below, i.e. as the linear system size L increases towards L_c . The aim of this paper is to analyze the behavior of the total energy of a dilute granular gas of hard spheres in that region, by using fluctuating hydrodynamics and the direct simulation Monte Carlo (DSMC) method [8]. A similar study for a system of hard disks, where the simulations were carried out by means of molecular dynamics, has already been reported elsewhere [9; 10].

2 Fluctuating hydrodynamics and average energy

One of the main advantages of the DSMC method [8] is that it allows to exploit the symmetry of the state to be investigated, when dividing the system into cells to apply the algorithm. For instance, to study average properties of the HCS, the system can be forced to stay homogeneous by considering a single cell, the position of the particles then becoming irrelevant. This allows to significantly increase the statistics of the results, decreasing the uncertainty. Of course, by doing this all the spatial hydrodynamic fluctuations and correlations that may occur in the system are by definition eliminated. This implies, in particular, that the clustering instability can not develop and its influence on the properties of the system can not be studied with a single cell.

Nevertheless, it is possible to consider intermediate situations where the clustering instability is present, but the system is forced to have some kind of symmetry that allows to increase the statistical accuracy. This can be achieved, in particular, by dividing the system into a given number of parallel layers of the same width. Each layer is considered as a cell when applying the DSMC algorithm. Since the positions of particles inside the same cell play no role in determining their collision probability, it follows that the dynamics is somehow coarse-grained over each layer and variations of the properties inside it can not be analyzed. On the other hand, variations of the hydrodynamic fields between different layers, i.e. along the coordinate perpendicular to them, can show up. Therefore, the clustering instability appears when the length of the system along that direction, L_x , reaches the critical value L_c . This is the coarse-grained description for which the theory will be developed in the following.

The total energy $\tilde{E}(t)$ of the system, either isolated or with periodic boundary conditions, we are considering can be expressed as

$$\begin{aligned} \tilde{E}(t) &\equiv \sum_{i=1}^N \frac{mV_i^2(t)}{2} \\ &= \int dx \left[\frac{3}{2} \tilde{N}_x(x, t) \tilde{T}(x, t) + \frac{m}{2} \tilde{N}_x(x, t) \tilde{u}^2(x, t) \right], \end{aligned} \quad (5)$$

where $\mathbf{V}_i(t)$ is the velocity of particle i at time t , the tilde is used to indicate that the quantities are treated as stochastic variables, and the x axis has been taken perpendicular to the layers described above. In the equation, $\tilde{N}_x(x, t)$ is the number of particles per unit of length in the x direction, $\tilde{\mathbf{u}}(x, t)$ is the flow velocity field, and $\tilde{T}(x, t)$ the temperature. The last two quantities are coarse-grained over the cells. The microscopic definitions of these fields are

$$\tilde{N}_x(x, t) = \sum_{i=1}^N \delta[x - X_i(t)], \quad (6)$$

$$\tilde{N}_x(x, t) \tilde{\mathbf{u}}(x, t) = \sum_{i=1}^N \mathbf{V}_i(t) \delta[x - X_i(t)], \quad (7)$$

$$\frac{3}{2} \tilde{N}_x(x, t) \tilde{T}(x, t) = \frac{m}{2} \sum_{i=1}^N [\mathbf{V}_i(t) - \tilde{\mathbf{u}}(x, t)]^2 \delta[x - X_i(t)], \quad (8)$$

that correspond to the idealized limit of infinitely narrow layers. Note that, consistently with the discussion above, only the x coordinate of the particles at time t , $X_i(t)$, appears in the definition of the coarse-grained fields. Expansion of Eq. (5) around the average values of the fields in the HCS, $Y_{\alpha, h}$, retaining up to second order terms in the deviations, $\delta\tilde{Y}_\alpha(x, t) \equiv Y_{\alpha, h} - \tilde{Y}_\alpha(x, t)$, yields

$$\begin{aligned} \delta\tilde{E}(t) &\equiv \tilde{E}(t) - E_h(t) \\ &= \frac{1}{2} \int dx \left\{ 3N_{x, h} \delta\tilde{T}(x, t) + 3\delta\tilde{N}_x(x, t) \delta\tilde{T}(x, t) \right. \\ &\quad \left. + mN_{x, h} [\delta\tilde{\mathbf{u}}(x, t)]^2 \right\}, \end{aligned} \quad (9)$$

with $E_h(t) \equiv 3NT_h(t)/2$ and $N_{x, h} \equiv N/L_x$.

In order to eliminate from the analysis the time dependence of the reference HCS, it is convenient to introduce dimensionless length ℓ and time s scales by

$$\ell = \frac{x}{\ell_0}, \quad ds = \frac{v_h(t) dt}{\ell_0}. \quad (10)$$

Also, dimensionless hydrodynamic fields are defined as

$$\rho_x(\ell, s) \equiv \frac{\delta\tilde{N}_x(x, t)}{N_{x, h}}, \quad (11)$$

$$\omega(\ell, s) \equiv \frac{\delta \tilde{\mathbf{u}}(x, t)}{v_h(t)}, \quad (12)$$

$$\theta(\ell, s) \equiv \frac{\delta \tilde{T}(x, t)}{T_h(t)}. \quad (13)$$

Moreover, the Fourier transform is introduced through

$$\rho_{x,k}(s) = \int d\ell e^{-ik\ell} \rho_x(\ell, s), \quad (14)$$

and similarly for the other fields. Then, Eq. (5) becomes

$$\begin{aligned} \epsilon(t) &\equiv \frac{\delta \tilde{E}(t)}{E_h(t)} \\ &= \frac{\theta_0(s)}{\Lambda_x} + \frac{1}{\Lambda_x^2} \sum_k \left[\rho_{x,k}(s) \theta_{-k}(s) + \frac{2}{3} |\omega_k(s)|^2 \right], \end{aligned} \quad (15)$$

with $\Lambda_x \equiv L_x/\ell_0$. Then, to calculate $\epsilon(t)$, expressions for the Fourier components of the fluctuating hydrodynamic fields are needed. It will be assumed that, at the mesoscopic level used here, they obey Langevin equations obtained by linearizing the Navier-Stokes equations for a granular gas around the HCS. Moreover, if attention is restricted to the quasi-elastic limit, i.e. α very close to unity, it can be expected that a good approximation be obtained by using the same expressions for the properties of the noise terms in the Langevin equations as those in the Landau-Langevin equations for normal fluids [11; 12].

Consider the Fourier transform of the flow field, $\omega_k(s)$. The vorticity field or transverse flow field in a general situation is by definition its component perpendicular to the vector \mathbf{k} , i.e. in the present case perpendicular to the x axis. It will be denoted by $\omega_{k,\perp}(s)$. The coarse-grained velocity field $\omega(\ell, s)$ is related with the actual velocity field $\mathbf{w}(\ell, s)$ by

$$\int d\ell_{\perp} \mathbf{w}(\ell, s) = \frac{V^*}{\Lambda_x} \omega(\ell, s), \quad (16)$$

where $\ell = \mathbf{r}/\ell_0$, ℓ_{\perp} denotes the vector component of ℓ perpendicular to the x axis, and V^* is the volume of the system in the dimensionless scale, $V^* = V/\ell_0^3$. Using this, it is easily obtained that the Landau-Langevin equation for $\omega_{k,\perp}(s)$ is

$$\left(\frac{\partial}{\partial s} - \frac{\zeta^*}{2} + \eta^* k^2 \right) \omega_{k,\perp}(s) = \xi_{k,\perp}^{(\omega)}(s). \quad (17)$$

The term $\xi_{k,\perp}^{(\omega)}(s)$ is a Gaussian white noise verifying the fluctuation dissipation relation

$$\langle \xi_{k,\perp}^{(\omega)} \xi_{k',\perp}^{(\omega)}(s') \rangle = \frac{\Lambda_x^2}{N} \delta(s-s') \delta_{k,-k'} \eta^* k^2 \mathbf{1}, \quad (18)$$

$\mathbf{1}$ being the unit tensor of dimension 2 and the angular brackets denoting average over the noise realizations. It is worth to remark that the clustering instability manifests itself in Eq. (17), which shows that for $|k| < k_c \equiv (\zeta^*/2\eta^*)^{1/2}$, the fluctuations of the scaled transverse flow

field grow in time. On the other hand, for $\Lambda_x < \Lambda_c = 2\pi/k_c$, the long time solution of Eq. (17) is

$$\omega_{k,\perp}(s) = \int_{-\infty}^s ds' e^{(s-s')\lambda_{\perp}(k)} \xi_{k,\perp}^{(\omega)}(s'), \quad (19)$$

with $\lambda_{\perp}(k) = \frac{\zeta^*}{2} - \eta^* k^2$. Then, by using Eq. (18) it is obtained:

$$\langle \omega_{k,\perp}(s) \omega_{k',\perp}(s') \rangle = -\frac{\Lambda_x^2 \eta^* k^2}{2N \lambda_{\perp}(k)} e^{(s-s')\lambda_{\perp}(k)} \delta_{k,-k'} \mathbf{1} \quad (20)$$

and, in particular,

$$\langle |\omega_{k,\perp}(s)|^2 \rangle = -\frac{\Lambda_x^2 \eta^* k^2}{N \lambda_{\perp}(k)}. \quad (21)$$

Equation (20) holds for $s > s' \gg 1$.

A Langevin equation for the energy is obtained by linearizing the macroscopic average equation for it,

$$\frac{d}{dt} \delta \tilde{E}(t) = -\frac{9}{4} \zeta_h(T_h) N_{x,h} \int dx \delta \tilde{T}(x, t). \quad (22)$$

For a normal fluid, the right hand side identically vanishes since the cooling rate is zero. Then, an equation for the scaled energy fluctuations is easily found,

$$\frac{d\epsilon(s)}{ds} - \zeta^* \epsilon(s) = -\frac{3\zeta^*}{2\Lambda_x} \theta_0(s). \quad (23)$$

The noise term mentioned above, intrinsic to the local energy dissipation in collisions, has been omitted, since it is expected to give small contributions as compared with those to be kept, in the quasi-elastic limit. Combination of Eqs. (15) and (23) yields

$$\begin{aligned} \frac{d\epsilon(s)}{ds} &= -\zeta^* \left\{ \frac{\epsilon(s)}{2} - \frac{3}{2\Lambda_x^2} \right. \\ &\quad \left. \times \sum_k \left[\rho_{k,x}(s) \theta_{-k}(s) + \frac{2}{3} |\omega_{k,\perp}(s)|^2 \right] \right\}, \end{aligned} \quad (24)$$

In the threshold of the clustering instability, the fluctuations of the transversal components of the flow velocity are expected to dominate over the density and the longitudinal velocity fluctuations, so the above equation can be reduced to

$$\frac{d\epsilon(s)}{ds} = -\frac{\zeta^*}{2} \left[\epsilon(s) - \frac{2}{\Lambda_x^2} \sum_k |\omega_{k,\perp}(s)|^2 \right]. \quad (25)$$

From this equation, it follows that the average value of the total energy of the system is

$$\langle \epsilon \rangle_{st} = \frac{2}{\Lambda_x^2} \sum_k \langle |\omega_{k,\perp}(s)|^2 \rangle_{st} = -\frac{2}{N} \sum_k \frac{\eta^* k^2}{\lambda_{\perp}(k)}. \quad (26)$$

This is the result expected from the expression obtained for a system without introducing the coarse-grain average over the parallel layers [10].

For $\widetilde{\delta L} \equiv (L_c - L_x)/L_c \ll 1$ and positive, the main contribution to Eq. (26) is given by those modes having the largest possible wavelength, i.e. those with $|k| = k_{min} = 2\pi/L_x$. For them, it is

$$\begin{aligned} \lambda_{\perp}(k) &= \lambda_{\perp}(k_{min}) = \frac{\zeta^*}{2} - \eta^* \left(\frac{2\pi}{L_x} \right)^2 \\ &= \frac{\zeta^*}{2} \left[1 - \left(\frac{L_c}{L_x} \right)^2 \right] \simeq -\zeta^* \widetilde{\delta L}. \end{aligned} \quad (27)$$

It is at this point when the coarse-grain used in the simulations deserves some attention. In a normal simulation, for instance using molecular dynamics of a cubic cell, the number of modes with $k = k_{min}$ compatible with the periodic boundary conditions should be 6, two for each of the axis of the system [10]. Nevertheless, the coarse-grain in the directions perpendicular to the layers, actually kills all the modes in those directions. Consequently only two modes with $k = \pm k_{min}$ survive. Then, from Eqs. (26) and (27),

$$\langle \epsilon \rangle_{st} = A_{\epsilon} (\widetilde{\delta L})^{-1}, \quad A_{\epsilon} = \frac{2}{N_{x,h} L_c}, \quad (28)$$

where it has been used that near the instability it is $N \simeq N_{x,h} L_c$. This equation shows that a renormalization by fluctuations of the total energy of the HCS takes place as the clustering instability is approached. In fact, it is seen that the energy of the system becomes larger than the prediction based on Haff's law. When interpreting this theoretical prediction, it must be kept in mind that the approximation carried out here only holds while the fluctuations are small as compared with their average values far from the instability. This requires, in particular, that the right hand side of Eq. (28) be small.

3 DSMC method results

The simulation results to be reported in the following have been obtained by using the DSMC method, partitioning the system in parallel layers as described above. The simulations started with a configuration in which the particles were homogeneously distributed along the length L_x of the system and their velocities obeyed a Maxwellian distribution. In order to increase the number of statistical averages and avoid the technical problems inherent to the continuous cooling of the HCS, the steady representation of the latter was used. This consists in a change in the time scale that implies a modification of the dynamics, but does not involve any internal property of the system. This dynamics leads to a steady state whose properties are exactly mapped into those of the HCS. The details of the method have been extensively analyzed elsewhere [13] and will be not repeated here. Then, the system is allowed to evolve until the steady state is reached. It is important to verify that the system has actually reached stationarity, since the

time required to reach it increases very fast as the instability is approached. For instance, for $\alpha = 0.9$, the system becomes stationary after about 100 collisions per particle for $L_x/L_c = 0.88$, while it needs of the order of 2000 collisions per particle for $L_x/L_c = 0.997$. Once the system is in the steady state, the different macroscopic properties of interest have been computed by taking averages of the microscopic values. In addition, in all the results reported here, the data have also been averaged over 1000 independent trajectories.

The height of the cells used in the simulations has been $\Delta x = 0.04\ell_0$, significantly smaller than the mean free path $\lambda = 0.225\ell_0$, as required by the DSMC method. The number of particles per cell was 100, so $N_{x,h} \equiv N/L_x = 2500\ell_0^{-1}$. The number of cells to be considered in each case was determined from the the above figures and the value of L_x being simulated. It is worth to stress that the number of particles does not affect the effective dynamics used in the DSMC that remains, by definition, that of an N particle system in the low density (Boltzmann) limit [8].

For a given value of α , the series of simulations were started with a system size L_x significantly smaller than the critical values predicted by Eq. (2), namely around 0.8 times that value. From there, the size of the system was increased systematically and its properties studied in each case. Special attention was given to verify the homogeneity of the hydrodynamic properties of the system. Once the formation of velocity vortices was observed, the series was stopped since this is the indication that the size is larger than the critical length L_c .

In Figs. 1 and 2 the quantity $\langle \epsilon \rangle_{st}^{-1}$ is plotted as a function of $L_x = L_x/\ell_0$ for $\alpha = 0.9$ and $\alpha = 0.8$, respectively. In both cases, an increase of the average energy relative to the Haff's law prediction is observed as the size of the system is decreased approaching the critical value. It must be noted, however, that this increase remains quantitatively small, namely below 10% in all the parameter region studied.

If the theoretical prediction in Eq. (28) is verified, the above plot must lead to a straight line, and that is in fact what is obtained when L_x increases approaching the critical length. This confirms the exponent -1 in Eq. (28). From the slope and the ordinate at the origin, the simulation values of the critical size L_c and the critical amplitude A_E are obtained. These fitting parameters as well as the theoretical predictions for them are given in Table 1. The theoretical prediction for the critical length has been obtained by means of Eq. (2) and the expressions for the shear viscosity and the cooling rate in the first Sonine approximation given in [7]. It is observed that the agreement between the theory and the simulation results for the critical size L_c is really good. This is consistent with the well established result that the first Sonine approximation provides good values for the shear viscosity and the cooling rate of a dilute granular gas in the range of values of α considered here.

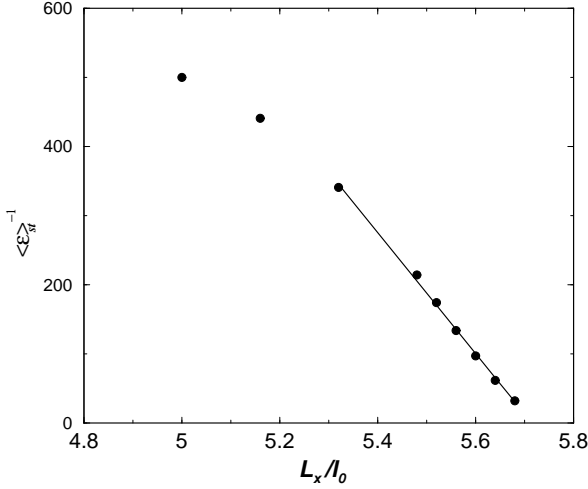


Fig. 1 Dimensionless quantity $\langle \epsilon \rangle_{st}^{-1}$, defined in the main text, as a function of the size of the system L_x , measured in units of $\ell_0 \equiv (n_h \sigma^2)^{-1}$, for $\alpha = 0.9$. The circles are the DSMC results and the solid line a linear fit near the clustering instability.

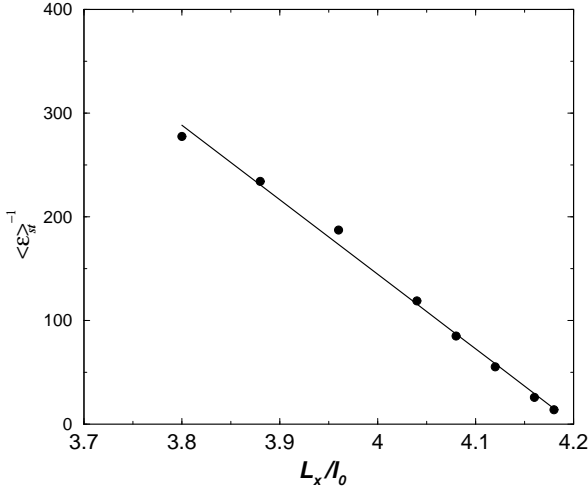


Fig. 2 The same as in Fig. 1, but for a system of particles with $\alpha = 0.8$.

On the other hand, the comparison between the theoretical prediction and the DSMC result for the critical amplitude of the energy A_ϵ is not so good. In Table 1 the measured values for $N_x L_c A_\epsilon$ is given. According to Eq. (28) it should be equal to a constant, independent of the inelasticity, namely 2. Instead, although the order of magnitude is accurately predicted, definitely larger values are obtained showing, in addition, a relevant dependence on α . Something about the possible origins of this discrepancy and the improvement of the theory will be said at the end of the paper.

Table 1 Theoretical prediction, $L_c^{(t)}$, and values obtained from the simulation data for the average energy, $L_c^{(\epsilon)}$, and from the second moment of the fluctuations, $L_c^{(\sigma)}$ for the critical length characterizing the clustering instability of a dilute three-dimensional granular gas, as a function of the coefficient of restitution α . In all cases, L_c is measured in units of $\ell_0 = (n_h \sigma^2)^{-1}$. The parameters reported in the last two columns involve the critical amplitudes A_ϵ and A_σ and should be both equal to 2, according to the theoretical predictions.

α	$L_c^{(t)}$	$L_c^{(s,\epsilon)}$	$L_c^{s,\sigma}$	$L_c^{(\epsilon)} N_x A_\epsilon^{(s)}$	$(A_\sigma^{(s)} N_x L_c^{(\sigma)})^2$
0.95	7.86	7.93	7.91	2.66	2.08
0.90	5.70	5.71	5.71	2.72	2.78
0.85	4.77	4.75	4.75	2.82	2.43
0.80	4.23	4.19	4.19	2.85	2.68
0.75	3.88	3.82	3.82	3.35	2.88

4 Critical energy fluctuations

Consider next the fluctuations around its average value of the total energy of the system, again in the threshold of the instability. Since it has been shown above that the average value of the energy differs from the Haff law prediction, let us define

$$\delta' \epsilon(s) \equiv \epsilon(s) - \langle \epsilon \rangle_{st} = \frac{\tilde{E}(s) - \langle \tilde{E}(s) \rangle}{E_H(s)}, \quad (29)$$

$$\delta' \bar{\omega}(s) \equiv \bar{\omega}(s) - \langle \bar{\omega}(s) \rangle_{st}, \quad (30)$$

with

$$\bar{\omega}(s) \equiv \frac{2}{\Lambda_x^2} \sum_k |\omega_{k,\perp}(s)|^2. \quad (31)$$

Equation (26) shows that $\langle \bar{\omega} \rangle_{st} = \langle \epsilon \rangle_{st}$ and, therefore, Eq. (25) is equivalent to

$$\frac{d}{ds} \delta' \epsilon(s) = -\frac{\zeta^*}{2} [\delta' \epsilon(s) - \delta' \bar{\omega}(s)]. \quad (32)$$

Taking into account that cumulants of $\omega_{k,\perp}$ of order higher than two vanish since $\xi_{\perp}^{(\omega)}(s)$ is assumed to be Gaussian, it follows from Eqs. (18) and (19) that

$$\langle \delta' \bar{\omega}(s) \delta' \bar{\omega}(s') \rangle = \frac{2}{N_{x,h}^2 L_c^2} e^{-2(s-s')\zeta^* \delta \tilde{L}} (\delta \tilde{L})^{-2}. \quad (33)$$

Upon deriving this equation, it has been used that only modes with \mathbf{k} in the direction of the x axis can be excited, due to the way in which the simulations are carried out. The solution of Eq. (32), once the initial value has been forgotten, is

$$\delta' \epsilon(s) = \frac{\zeta^*}{2} \int_{-\infty}^s ds_1 e^{-\zeta^*(s-s_1)/2} \delta' \bar{\omega}(s_1). \quad (34)$$

Then, by means of Eq. (33) it follows that

$$\begin{aligned} \langle \delta' \epsilon(s) \delta' \epsilon(s') \rangle &= \frac{2}{N_{x,h}^2 L_c^2} e^{-2(s-s')\zeta^* \delta \tilde{L}} (\delta \tilde{L})^{-2} \\ &= \langle \delta' \bar{\omega}(s) \delta' \bar{\omega}(s') \rangle, \end{aligned} \quad (35)$$

$s \geq s' \gg 1$. Terms involving powers of $\widetilde{\delta L}$ larger than -2 have been consistently neglected in this expression. Thus both the total energy fluctuations and the fluctuations of the energy associated with the transversal modes decay with a characteristic time $(2\zeta^* \widetilde{\delta L})^{-1}$, indicating a divergent behavior of the relaxation time as $\widetilde{\delta L}^{-1}$. Also, the second moment of the energy fluctuations is predicted to diverge. For $s = s'$, Eq. (35) leads to the stationary value

$$\langle (\delta' \epsilon)^2 \rangle_{st} = A_\sigma^2 \widetilde{\delta L}^{-2}, \quad A_\sigma = \frac{\sqrt{2}}{N_{x,h} L_c}. \quad (36)$$

It is

$$\sigma_E^2 \equiv \frac{\langle (\widetilde{E}(s) - \langle \widetilde{E}(s) \rangle)^2 \rangle}{\langle \widetilde{E}(s) \rangle} \simeq \langle (\delta' \epsilon)^2 \rangle. \quad (37)$$

To compare with the DSMC method results, it must be realized that Eq. (36) gives the moment of the energy fluctuations that dominate near the instability, but in a region where the fluctuations are still small. Then, what has been done is to measure σ_E^2 as a function of L_x , starting from values quite smaller than L_c . There, the value of σ_E is not affected by the presence of the instability, and $N\sigma_E^2$ is independent of L_x [3]. It will be denoted by $(N\sigma_E^2)_h$. Then, the quantity considered has been

$$\psi \equiv \left[\frac{N_{x,h} L_c \sigma_E^2}{(N\sigma_E^2)_h} - 1 \right]^{-1/2}. \quad (38)$$

The measured values for this quantity are plotted as a function of L_x in Figs. 3 and 4, for $\alpha = 0.9$ and $\alpha = 0.8$, respectively. As predicted by Eq. (36), a linear behavior is observed as the critical size is approached. Although the fit is reasonably good for all the values of α reported here, it becomes clearly worse as the inelasticity increases. Moreover, the ‘critical’ region, identified by the values of L_x for which the predicted qualitative critical behavior is actually observed, is smaller for the second moment of the energy than for its average. This can be verified by comparing, for instance, Figs. 2 and 4. In contrast to what happened with the average energy, the growth exhibited by the fluctuations is quite fast. In the region plotted in Figs. 3 and 4, the second moment σ_E increases more than one order of magnitude.

From the slope and ordinate in the origin of the fitting straight line, the simulation values of the critical length L_c and amplitude A_σ are directly derived. The values obtained in this way are also included in Table 1. Again, the results for the critical length L_c are in excellent agreement with the theoretical predictions. Moreover, the fact that the same values follow from the measurements of both the average energy and the second moments provides a test of the internal consistency of the theory. With regard to the critical amplitude A_σ , significant deviations from the theoretical predictions are also found in this case, although they are smaller than for A_c . In fact, for the most elastic system considered,

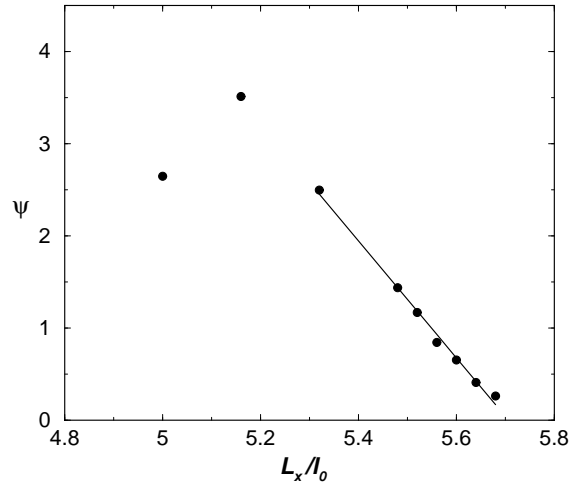


Fig. 3 Plot of the DSMC results (circles) for the dimensionless quantity defined in Eq. (38) as a function of the size of the system L_x , for $\alpha = 0.9$. The solid line is a linear fit near the clustering instability.

$\alpha = 0.95$, there is a good agreement. The most relevant disagreement between theory and simulations is the definite dependence on inelasticity of the parameter combination given in Table 1 shown by the latter, while the former predicts a constant value (namely, 2).

It can be wondered which is the aspect of the theoretical approach developed here that should be modified in order to improve the accuracy of the predicted expressions for the critical amplitudes. Of course, a first important limitation of the theory is its restriction to the almost elastic limit, implied by the use of the Landau fluctuation-dissipation relations. But it must be realized that up to now those expressions have not been generalized for non-conservative interactions. A more modest step in this direction should be to include in Eq. (22) the intrinsic noise term associated with the cooling rate, as already indicated.

In refs. [9] and [10], a scaling property of the probability distribution of the energy fluctuations in the threshold of the clustering instability of a two-dimensional granular fluid was identified. Moreover, the scaling function was very well fitted by the same expression as found in several equilibrium and non-equilibrium molecular systems [14; 15]. The possible existence of a similar scaling for the three-dimensional granular gas considered here has also been investigated, finding similar results.

Acknowledgements This research was supported by the Ministerio de Educación y Ciencia (Spain) through Grant No. FIS2005-01398 (partially financed by FEDER funds).

References

1. Haff PK (1983) Grain flow as a fluid mechanical phenomenon. *J. Fluid Mech.* 134:401-430.

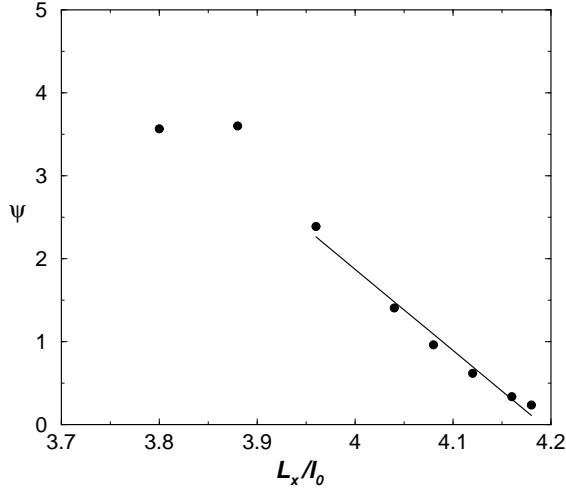


Fig. 4 The same as in Fig. 3, but for $\alpha = 0.8$.

2. Goldman DI, Swift JB, and Swinney HL (2004) Noise, coherent fluctuations, and the onset of order in an oscillated granular fluid. *Phys. Rev. Lett.* 92:174302-1,-4.
3. Brey JJ, García de Soria I, Maynar P, and Ruiz-Montero MJ (2004) Energy fluctuations in the homogeneous cooling state of granular gases. *Phys. Rev. E* 70:011302-1,-12.
4. Visco P, Puglisi A, Barrat A, van Wijland F, and Trizac E (2006) Energy fluctuations in vibrated and driven granular gases. *Eur. Physics J. B* 51:377-389.
5. Goldhirsch I and Zanetti G (1993) Clustering instability in dissipative gases. *Phys. Rev. Lett.* 70:1619-22.
6. Brey JJ, Ruiz-Montero MJ, and Cubero D (1999) Origin of density clustering in a freely evolving granular gas. *Phys. Rev. E* 60:3150-3157.
7. Brey JJ, Dufty JW, Kim CS, and Santos A (1998) Hydrodynamics for granular flow at low density. *Phys. Rev. E* 58:4638-4653.
8. Bird G (1994) *Molecular Gas Dynamics and the Direct Simulations of Gas Flows*. Clarendon Press, Oxford.
9. Brey JJ, García de Soria MI, Maynar P, and Ruiz-Montero MJ (2005) Scaling and Universality of Critical Fluctuations in Granular Gases. *Phys. Rev. Lett.* 94:098001-1,-4.
10. Brey JJ, Domínguez A, García de Soria MI, and Maynar P (2006) Mesoscopic Theory of Critical Fluctuations in Isolated Granular Gases. *Phys. Rev. Lett.* 96:158002-1,-4.
11. Landau L and Lifshitz EM (1959) *Fluid Mechanics*. Pergamon Press, New York.
12. van Noije TPC, Ernst MH, Brito R, and Orza JAG (1997) Mesoscopic Theory of Granular Fluids. *Phys. Rev. Lett.* 79:411-414.
13. Brey JJ, Ruiz-Montero MJ, and Moreno F (2004) Steady-state representation of the homogeneous cooling state of a granular gas. *Phys. Rev. E* 69:051303-1,-13.
14. Bramwell ST, Holdsworth PCW, and Pinton J-F (1998) Universality of rare fluctuations in turbulence and critical phenomena. *Nature* 396:552554.
15. Bramwell ST, Christensen K, Fortin J-Y, Holdsworth, Jensen HJ, Lise S, López JM, Nicodemi M, Pinton J-F, and Sellito M (2000) Universal fluctuations in correlated systems. *Phys. Rev. Lett.* 84:3744-3748.